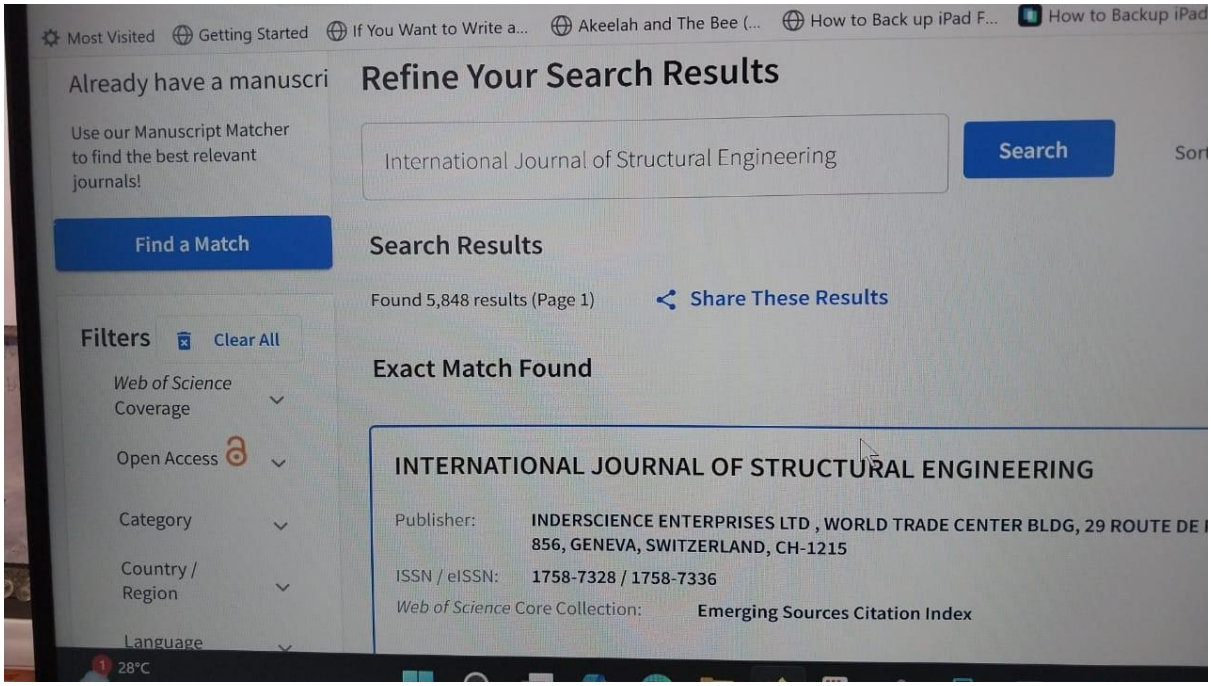
Most Visited
Getting Started
If You Want to Write a...
Akeelah and The Bee (...
How to Back up iPad F...
How to Backup iPad
Already have a manuscri
Use our Manuscript Matcher to find the best relevant journals!
Find a Match
Refine Your Search Results
International Journal of Structural Engineering
Search
Sort
Search Results
Found 5,848 results (Page 1)
Share These Results
Filters
Clear All
Web of Science Coverage
Open Access
Category
Country / Region
Language
Exact Match Found
INTERNATIONAL JOURNAL OF STRUCTURAL ENGINEERING
Publisher:
INDERSCIENCE ENTERPRISES LTD , WORLD TRADE CENTER BLDG, 29 ROUTE DE
856, GENEVA, SWITZERLAND, CH-1215
ISSN / eISSN:
1758-7328 / 1758-7336
Web of Science Core Collection:
Emerging Sources Citation Index
28°C

Passive Seismic Protection of Shear Building Using Shape Memory Alloy-Based Tension Sling Damper

Sujata H Mehta* amd Sharadkumar Purohit**

Passive control force is obtained from Shape Memory Alloy-based Tension Sling Damper (SMA-TSD) fitted to a seismically excited 10 storeyed shear building. One-dimensional Tanaka model is considered to represent the hysteresis behavior of SMA-TSD. This exhibits a nonlinear relationship between damper force and input states; hence, its implementation with linear system is a non-trivial task. In the paper, SMA-TSD is represented by Voigt model comprising equivalent stiffness and damping components derived by mapping it with flag-shaped hysteresis loop defined by Tanaka model. The results for controlled response of the buildings are obtained in terms of peak response quantities, i.e., interstorey drift, displacement and acceleration. One SMA-TSD fitted at ground storey of the building yields moderate control (4 29%) in peak response quantities. However, peak response quantities reduce substantially (4 53%) for different levels of El Centro seismic excitations and moderately (4 19%) for 50% Kobe seismic excitation when two SMA-TSDs are used in the building. The efficacy of SMA-TSD implemented in the study is a function of design parameters, diameter of SMA wire and length of SMA wire, and can be optimized.

Author pls chk: symbols are missing

Keywords: Shape Memory Alloy (SMA), Tension Sling Damper (TSD), Voigt model, Passive control

Introduction

Seismic response of buildings has been a matter of utmost concern in order to save lives and minimize damages amid fast paced growth of vertical cities. Some design strategies, including base isolation and supplemental damping devices, are frequently practiced in seismic-prone areas. Base isolation increases the natural period of the overall structure, which reduces its acceleration response under seismic excitation, and thus it works efficiently for stiff structures (Housner *et al.,* 1997). For other types of structures, primary damping mechanisms are activated through passive energy dissipation devices like viscous fluid dampers, viscoelastic solid dampers, metallic dampers and friction dampers (Soong and Spencer, 2002). These

* Research Scholar, Department of Civil Engineering, School of Engineering, Institute of Technology, Nirma University, Ahmedabad 382481, Gujarat, India; and is the corresponding author. E-mail: 13extphde106@nirmauni.ac.in

** Professor, Department of Civil Engineering, School of Engineering, Institute of Technology, Nirma University, Ahmedabad 382481, Gujarat, India. E-mail: sharad.purohit@nirmauni.ac.in

Author pls confirm information

devices dissipate energy resulted due to seismic excitation of the system in the form of heat due to viscous friction in viscous fluid damper, yielding of metal in metallic damper, shearing of viscoelastic material in viscoelastic damper and sliding friction between two surfaces in friction damper (Pall and Marsh, 1982; Aiken and Kelly, 1992; and Symans and Constantinou, 1998). The aim of such devices in a structure is to limit damaging deformations, but the extent to which a particular device accomplishes the aim depends on the inherent properties of the structure, properties of damping device and characteristics of seismic excitations (Symans *et al*., 2008).

Advent of smart materials with controllable inherent properties paves the way for the development of structure with real-time control. Various classes of dampers known as semi-active, active and hybrid dampers have been developed and implemented with structures to control structural response due to wind or seismic excitation. First ever application of active control of structure was presented by Sae-Ung and Yao (1978). However, due to requirement of capital energy and long-term reliability concerns, a class of dampers, known as semi-active dampers, have become increasingly popular. These dampers are regarded as controllable passive devices as relative motion between their ends are resisted passively but with controllable mechanical properties (Spencer and Nagarajaiah, 2003). Viscous-orifice dampers, electrorheological dampers and magnetorheological dampers are a few examples of controllable passive devices (Jansen and Dyke, 1999; and Chen *et al.*, 2004). Despite the presence of semi-active dampers and active dampers as design strategy for existing and new structures, passive energy dissipation devices are being used due to their robustness and cheaper cost.

Shape Memory Alloys (SMA) are relatively new class of materials, having unique controllable characteristics of shape memory effect and super-elasticity, qualifying it as smart materials. Superelasticity property of SMA material enables it to undergo stress induced hysteretic phase transformation from parent austenite phase to martensite phase and vice versa without inducing any residual strain (Buehler and Wiley, 1961). Super-elastic SMA materials are capable of repeatedly absorbing large amounts of energy under loading cycles without exhibiting permanent deformation (Ozbulut *et al.*, 2011). Jani *et al.* (2014) presented an exhaustive review on SMA material focused on research and application of SMA. Various forms or types of SMA include NiTi SMA, High Temperature SMAs (HTSMA), Magnetic SMAs (MSMAs), SMA thin film and Shape Memory Alloy Polymers (SMPs). However, the present research mostly concentrates on application of NiTi SMAs to seismic control of buildings. Various researchers performed experimental investigations to characterize nonlinear hysteresis behavior or NiTi SMAs and provided constitutive relationships (Tanaka, 1986; Graesser and Cozzarelli, 1991; Schmidt, 2006; and Ren *et al*., 2007).

Improved damping characteristics and added stiffnesses offered by SMA when strained due to input motion make it a potential contender for developing passive,

semi-active and hybrid control devices to control the structural response of a variety of problems (Jani *et al.*, 2014). Recently, many applications of SMA-based passive and hybrid control devices to control seismic response of various structures have been found in the literature. Dolce *et al.* (2005) and McCormik *et al.* (2006) developed passive dampers using SMA wires and implemented them with Reinforced Concrete (RC) frames. Similar application of SMA-based passive damping devices with steel frame was studied by Mortazavi *et al.* (2013) and as Buckling Restrained Braces (BRBs) with steel frame was studied by Miller *et al.* (2012). Zhang and Zhu (2007) implemented passive SMA wire-based damper with benchmark nonlinear problem and demonstrated that SMA damper is a function of wire diameter, strain rate, amplitude and pre-straining of SMA wire.

The paper implements passive SMA wire-based Tension Sling Damper (TSD) with 10 storey shear building of Yuen *et al.* (2007) subjected to seismic excitations. The efficacy of SMA-TSD used in the study is established through seismic response quantities, i.e., peak displacement, peak acceleration, peak inter storey drift and peak damper force. Nonlinear hysteretic behavior of SMA-TSD is modeled with simplified Tanaka model without considering its strain rate dependency. Viscoelastic material-based linear Kelvin-Voigt model is used to represent nonlinear hysteresis behavior of SMA-TSD and is characterized as equivalent linear model with equivalent stiffness and damping under seismic excitation (Sun and Lu., 1995). Seismic response control for model based 10 storey building is determined employing one SMA-TSD device at ground floor and two SMA-TSD devices and ground floor and first floor/ second floor of the building (Figure 1).

Figure 1: Ten-Storey Building

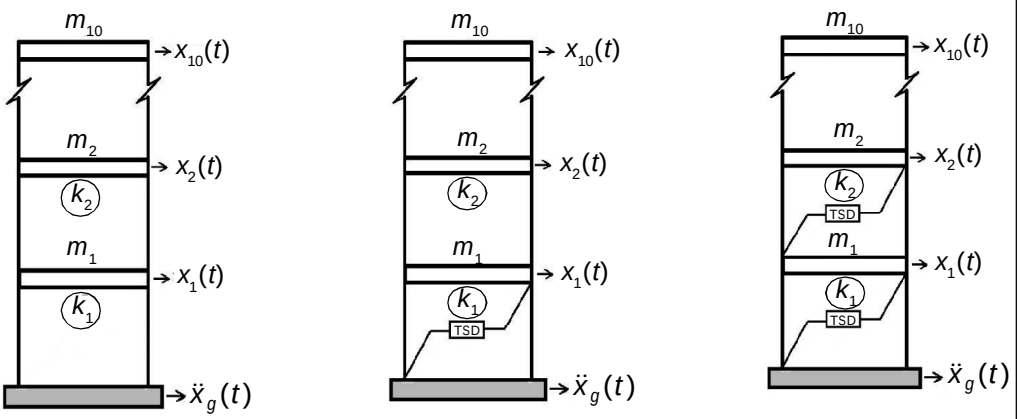

(a) Uncontrolled (b) Controlled with one TSD (c) Controlled with two TSD

2. Methodology

2.1 Ten-Storey Building

A ten-storey building represented as plane frame with rigid floors is modeled as lumped mass system with one degree of freedom at each storey level, as shown in Figure 1a. The same building controlled by one damper at ground floor and two dampers at ground and first floor are shown in Figure 1b and Figure 1c, respectively, under seismic excitations (Yuen *et al*., 2007). The equation of motion for the building is expressed as:

$$M\ddot{x}(t) + C\dot{x}(t) + Kx(t) = Gf - ML\ddot{x}_g(t) \quad \ldots(1)$$

where M is the mass matrix given as diag $[m_i]$ of nominal mass of each storey m_i = 50 kg, K is tridiagonal stiffness matrix with $K_{ii} = k_i + k_{i+1}$, $k_{i,\,i+1} = -k_{i+1}$, $k_{i,\,i-1} = k_{i-1}$, where k_i is interstorey stiffnesses given as 948.70, 836.99, 886.11, 889.33, 925.77, 881.83, 833.79, 824.03, 872.11 and 829.86 N/cm for i = 1,2,...10, first to tenth storey, respectively. Damping coefficient matrix C is derived from proportional (Rayleigh) damping coefficients α_m = 0.1 s^{-1} and α_k = 7.36 × 10^{-4} s as $C = \alpha_m M + \alpha_k K$ with 1% damping ratio for first two modes [23]. The effect of seismic excitations at each storey is given as influence matrix L, which is a unit column matrix. Seismic ground acceleration is denoted as $\ddot{x}_g$ and $x = [x_1\ x_2..x_{10}]^T$ is the displacement vector for 10 storeys measured relative to the ground. G is the location matrix indicating damper/s location and f is the control force vector. For uncontrolled system G is null matrix, for one damper G is $[-1\ 0\ 0\ \ldots 0]^T$ and $f = f_1$. For the two-damper case: G is a two-column matrix with $G_{ij} = 0$ except $G_{11} = G_{22} = -G_{12} = -1$, and $f = [f_1\ f_2]^T$, where each damper is at ground and first floor. For two-damper case, where one damper is at ground and the other damper at third floor, G is a two-column matrix with $G_{ij} = 0$ except $G_{11} = G_{32} = -G_{22} = -1$. If the building is modeled as a plant with states defined as $z = [x\ \dot{x}]^T$ and the output vector $y = [\ddot{x}_1\ \ddot{x}_2 \cdots \ddot{x}_{10}\quad x_1\ x_2 \cdots x_{10}]$ the state and output equations are described in Equations (2) and (3), respectively.

Author pls chk and confirm [23]

Author pl. check symbol is missing

$$\dot{z} = Az + Bf + Ex_g \quad \ldots(2)$$

$$y = Cz + Df \quad \ldots(3)$$

where A is system matrix, B is input matrix, C is output matrix, D is direct transmission matrix and E is location matrix for seismic excitations, and f is control force vector.

$$A = \begin{bmatrix} 0 & I \\ -M^{-1}K & -M^{-1}C \end{bmatrix};\ B = \begin{bmatrix} 0 \\ M^{-1}G \end{bmatrix};\ E = -\begin{bmatrix} 0 \\ L \end{bmatrix}$$

$$C = \begin{bmatrix} -M^{-1}K & -M^{-1}C \\ I & 0 \end{bmatrix};\ D = \begin{bmatrix} -M^{-1}G \\ 0 \end{bmatrix}$$

2.2 Tension Sling Damper

TSD comprises SMA slings of NiTinol wires developed to induce passive damping force. Figure 2a shows the plan of the TSD prototype with its components and Figure 2b provides side elevation of the TSD for completeness. TSD design includes proportioning of SMA wire diameter, total area represented by number of SMA slings and length of SMA sling. These parameters in the study are determined through a number of iterations corresponding to seismic excitation. The making principle of TSD is represented in Figure 2c and Figure 2d for back and forth motion induced due to input motion resulted into tensile strain only in one of the sets of SMA slings that remain engaged, while other set is disengaged. Design parameters of TSD are

Figure 2: Details of Tension Sling Damper

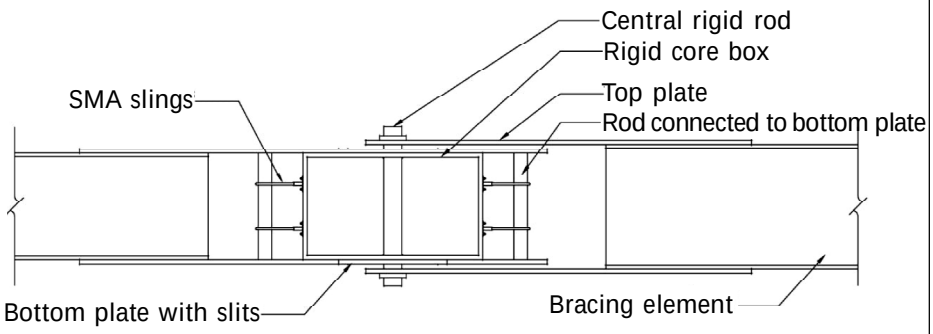

(a) Plan of TSD with nomenclature

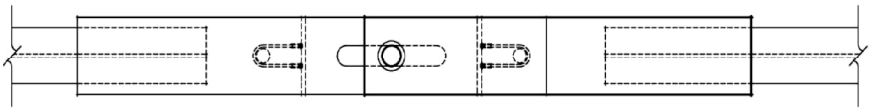

(b) Side elevation of TSD

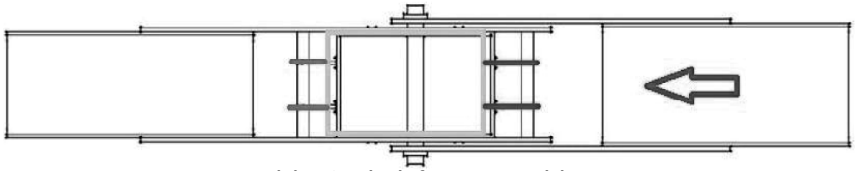

(c) TSD in left sway position

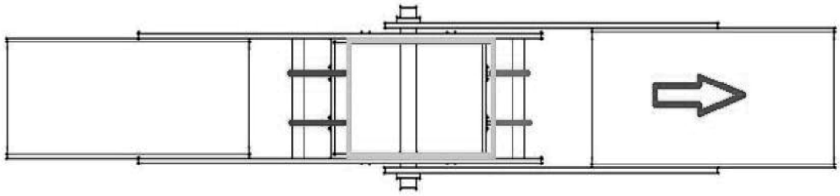

(d) TSD in right sway position

identified to limit operating strain level within 6 to 8% and thus TSD will not show any permanent offset. It can be fairly assumed that TSD will be recentered when velocity changes its sign.

Mechanical properties of NiTinol considered for SMA slings are modulus of elasticity for martensite (E_M) and austenite (E_A)—46 GPa and 55 GPa, austenite start and finish temperature –3 °C and 7 °C, martensite start and finish temperature –28 °C and –43 °C. Stress influence coefficients for martensite and austenite are C_M and C_A are 7.4 MPa/°C (Hartl and Lagoudas, 2008). Design parameter identification process reveals that smaller diameter of SMA wire is most likely to undergo phase transition from austenite to martensite due to presence of large magnitude of strain, inducing energy dissipation leading to increased damping. On the other hand, larger diameter SMA wire limit its contribution to stiffness. The design diameter for SMA wires used for SMA-TSD derived for the study is of the order 0.58 mm and lower. Such SMA wires, when rolled against rigid rod to form SMA sling, as shown in Figure 2a, bears finite contact and likely to offer negligible friction force in low velocity regime.

However, if strap of SMA wire is considered instead of small diameter SMA wire-based sling, frictional force may be generated at point of contact when velocity of input motion tends to zero. This shall be accounted for in the modeling of SMA-TSD. Additional damping supplemented by SMA-TSD is found within the range of 13 to 21% due to seismic excitation for the design parameters considered in the study which is comparable with other supplemental passive damping devices. The passive TSD is fitted in position within the principal diagonal in the ten-storeyed shear building at ground floor and first floor. The other possible configuration of TSD placement is horizontal position with chevron bracing.

2.3 Characterization of SMA-Based TSD

Passive control force of TSD can be evaluated from constitutive relationship between stress, strain and temperature developed by various researchers. Tanaka (1986) proposed one-dimensional stress-strain-temperature dependent model with exponential equation for kinematic phase transformations for SMA wires which was modified by Liang and Rogers through cosine function (Liang and Rogers, 1997). These models were strain-rate independent and thus other models such as Boyd and Lagoudas's thermodynamic model and Schmidt's plasticity model focused on strain-rate dependence that resulted into complex expressions and were practically non-implementable (Boyd and Lagoudas, 1996; and Schmidt, 2006). Graesser and Cozzaraelli developed strain-rate dependent one-dimensional model, more commonly known as G-C model, which is a modified form of Bouc-wen model given by Ozdemir to characterize nonlinear hysteresis behavior of SMA wires. Ren *et al.* (2007)further modified G-C model with different model parameters for different loading branches (Ozdemir, 1976; and Graesser and Cozzaraelli, 1991).

Owing to simplicity and versatility, the study considers one-dimensional Tanaka model for SMA-based TSD with constitutive relationship as:

$$\sigma = [E_A + \xi (E_M - E_A)]\,[\varepsilon - \xi H^{cur}(\sigma)] \quad ...(4)$$

where martensitic volume fraction is evaluated as:

$$\xi = 0 \text{ if } T \geq M_s^{\sigma} \text{ or } T \geq A_f^{\sigma};\ \xi = \frac{(M_s^{\sigma} - T)}{(M_s - M_f)} \text{ if } M_s^{\sigma} < T < M_s^{\sigma};$$

$$\xi = \frac{(A_f^{\sigma} - T)}{(A_f - A_s)} \text{ if } A_s^{\sigma} < T < A_f^{\sigma};\ \xi = 1 \text{ if } T \leq M_f^{\sigma} \text{ or } T \leq A_s^{\sigma}$$

where $H^{cur}(\sigma)$ = maximum transformation strain, E_A = Elastic modulus of austenite and E_M = Elastic modulus of martensite, σ = mechanical stress and ε = total strain in SMA wire, A_s, M_s, A_s and A_f are austenite and martensite start and finish temperatures respectively, which modifies in the presence of stress as:

$$A_s^{\sigma} = A_s + \frac{\sigma}{C_A};\ M_s^{\sigma} = M_s + \frac{\sigma}{C_M};\ A_f^{\sigma} = A_f + \frac{\sigma}{C_A};\ M_f^{\sigma} = M_f + \frac{\sigma}{C_M}.$$

SMA-based damper device with nonlinear hysteresis behavior when fitted with a discrete linear dynamic system warrants nonlinear dynamic analysis to be performed to evaluate response quantities. Since nonlinear dynamic analysis is computationally intensive and time-consuming due to its iterative nature, day-to-day design strategies prefer linear dynamic analysis instead. Various seismic codes recommend use of equivalent linear model for SMA-based control devices mapping accurately its nonlinear hysteretic behavior (AASHTO, 1991). One such example of equivalent linear damping model is given by Ghodke and Jangid (2016) wherein stiffness and damping components of SMA-based energy dissipation devices were determined through energy equivalence.

In the paper, TSD mechanism is cyclic tensile stress that resembles well with experimental investigations carried out on SMA wire and thus its behavior depends on loading history (Tanaka, 1986; Zhang and Zhu, 2007; and Hartl and Lagoudas, 2008). Therefore, SMA wire with hysteretic behavior can be termed as a viscoelastic material and falls within the scope of linear theory. Hysteretic behavior of such material can be represented by the Voigt model which comprises stiffness and damping components, parallelly (Sun and Lu, 1995). The force displacement relationship for Voigt model for SMA-based TSD is given in Equation (5) as:

$$F_{SMA} = k_{eq}\, x(t) + C_{eq}\dot{x}(t) \quad ...(5)$$

where F_{SMA} = force produced by SMA-based TSD; k_{eq} = equivalent stiffness of SMA wire and C_{eq} = equivalent damping of SMA wire.

Equivalent linear stiffness and damping parameters derived in Equation (5) for SMA-based TSD are determined following AASHTO guidelines for SMA material used for base isolation. Figure 3a shows force-displacement schematic diagram of flag-shaped one-dimensional Tanaka model for SMA-TSD and its conversion to viscoelastic Voigt model with co-ordinates of maximum, minimum—force and—displacement. Equivalent stiffness parameter of Voigt model, derived in Equation (5), can be evaluated as:

$$k_{eq} = \frac{(F_{max} - F_{min})}{(x_{max} - x_{min})} \qquad ...(6)$$

where F_{max} and F_{min} are maximum and minimum force induced by TSD, x_{max} and x_{min} are maximum and minimum displacement observed by TSD under the input motion.

Figure 3: Characterization of SMA Based Passive TSD

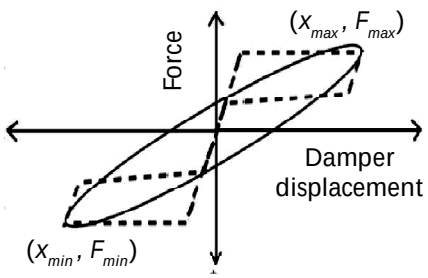

(a) Schematic diagram for flag-shaped SMA conversion to viscoelastic Voigt model

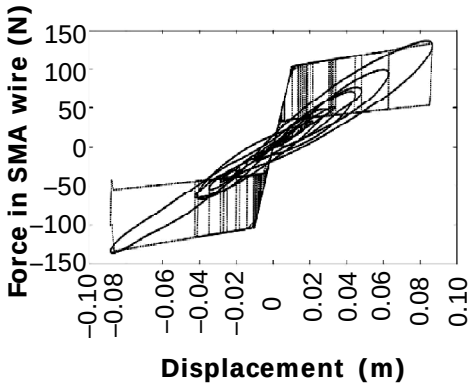

(b) Equivalent linear Voigt model for Kobe (50%) seismic excitation

The equivalent viscous damping, c_{eq} expresses energy dissipation capacity of the super-elastic SMA wire due to cyclic inelastic deformation is given as:

$$c_{eq} = 2\xi_{eq}\sqrt{k_{eq}\, m} \qquad ...(7)$$

where ξ_{eq} is the equivalent viscous damping ratio and m is mass of the storey when SMA-based TSD is fitted. Equivalent viscous damping ratio ξ_{eq} can be expressed as work done by damper force per cycle as:

$$\xi_{eq} = \frac{W_D}{2\Pi k_{eq} x_{\max}^2} \quad \ldots(8)$$

where W_D is energy dissipated by the damper force per cycle of hysteretic SMA-based TSD. Energy dissipated by the damper force per cycle within the flag-shaped hysteresis loop of SMA wire is determined from known co-ordinates of SMA NiTinol wire at ambient temperature, as shown in Figure 3b. Representation of SMA-based TSD by the Voigt model of two components is validated by comparing energy dissipated by the flag-shaped hysteresis loop with the viscoelastic hysteresis loop.

Energy dissipated by the damper force for both types of hysteresis loops (refer Figure 3b) is found to be about 10.85 J for design parameters of SMA wire; 0.58 mm diameter, 1.45 m length and 50 kg mass of the system under Kobe displacement time history excitation. Figure 3b shows comparison of flag-shaped hysteresis loop of SMA wire with viscoelastic Voigt model hysteresis loop. The maximum strain rate of SMA-based TSD considered is found to be 14.08 mm/min under Kobe seismic excitation. It has been established from experimental investigations on SMA wire subjected to reverse cyclic loading that within the range of strain rate of 10 mm/min to 15 mm/min, the damping capability of SMA wire does not reduce but marginally increases (Ren *et al*., 2007; and Fan *et al*., 2019). In the study, lower bound value of damping for a given strain rate is considered and thus the damping capability estimated for SMA-TSD is slightly conservative.

3. Results and Discussion

The efficacy of SMA-based TSD towards controlling seismic response of a ten-storey shear building is studied under different magnitudes of classical seismic excitations, for e.g., strong motion type El Centro seismic excitations record (1940) of levels 50%, 100% and 150% and pulse type Kobe seismic excitation (1995) of 50% record are considered in the study. The Kobe seismic excitation is considered with half of its original acceleration amplitude to avoid unreasonably high response of the building if subjected to unscaled time history since PGA (Peak Ground Acceleration) of unscaled Kobe seismic excitation is about 2.4 times larger than that of unscaled El Centro seismic excitation. Two cases are considered, in which ten-storey shear building is fitted with single SMA-based TSD at ground floor and in second case, same building is fitted with two identical SMA-based TSD at ground and first floor and at ground floor and third floor. Location of SMA-based TSD is determined based on interstorey drift response of uncontrolled case, i.e., ten-storey shear building without SMA-based TSD which is similar to other studies (Yuen et al., 2007, Purohit and Chandiramani, 2012). Uncontrolled response of ten-storey building without SMA-based TSD is evaluated from Equation (2) with null matrix *G* under different seismic excitations. The results of uncontrolled response for ten-storey shear building are compared with the reported results of Yuen *et al.* (2007) for validation (Table 1).

Table 1: Comparison of Uncontrolled Response of Ten-Storey Shear Building

Seismic Response Quantities	Seismic Excitations							
	El Centro				Kobe			
	50%		100%		150%		50%	
	Yuen *et al.*	Present Study	Yuen *et al.*	Present Study	Yuen *et al.*	Present Study	Yuen *et al.*	Present Study
peak displacement (cm)	11.830	11.810 (–0.17)	23.66	23.620 (–0.17)	35.495	35.430 (–0.18)	29.180	29.120 (–0.21)
peak interstorey drift (cm)	1.816	1.810 (–0.33)	3.632	3.620 (–0.33)	5.447	5.430 (–0.31)	5.443	5.420 (–0.42)
peak acceleration (g)	0.566	0.562 (–0.71)	1.133	1.123 (–0.89)	1.699	1.685 (–0.83)	1.909	1.892 (–0.90)

Controlled responses of ten-storey shear building fitted with—one and two—SMA-TSD are evaluated utilizing Equation (2) to Equation (8). Note that control damper force of SMA-TSD FSMA in Equation (6) is denoted as force vector *f* in Equation (2). Control damper force by SMA-TSD is determined from mechanical properties, as mentioned in section 2.2 and one-dimensional Tanaka model at ambient temperature of 25° C. SMA-TSD is fitted in the principal diagonal connecting ground storey and first-storey for one-damper case. For two-damper case, SMA-TSD connects ground storey and first-storey; as well as first and second storey when ten-storey building is subjected to El Centro seismic excitations. SMA-TSD in two-damper case of the building subjected to Kobe seismic excitation connects ground storey and first storey and second storey and third storey to achieve reasonably controlled seismic response.

3.1 Controlled Building with One SMA-TSD

Controlled seismic response of the ten-storey shear building fitted with one SMA-TSD, as shown in Figure 1b, is represented in terms of seismic response parameters, peak displacement, peak interstorey drift, peak acceleration and peak damper force. Design parameters: length, diameter and number of SMA wire sling are determined through iterative search method. Table 2 shows seismic response parameters of ten-storey shear building fitted with SMA-TSD/s. Bracketed quantity denotes percentage difference between uncontrolled and controlled response where –ve indicates reduction. It has been found that one SMA-TSD yields moderate peak displacement reduction (up to 27%) for ten-storey building for all levels for El Centro seismic excitations. However, peak displacement response remains marginally higher (up to 6%) for the ten-storey building with one TSD under Kobe seismic excitation. Peak interstorey drift shows uniform reduction up to 4 19% for ten-storey building with one SMA-TSD as compared to its uncontrolled response for all seismic excitations. One SMA-TSD is found to be effective in reducing peak acceleration up to 4 11% for all

Author pl. check: symbols are missing

Table 2: Seismic Response Parameters of Controlled Ten-Storey Building with One and Two SMA-TSD

Seismic Excitations	Ten-Storey Building	TSD Design Parameters[1]	Peak Displacement (m)	Peak Interstorey Drift (m)	Peak Acceleration (m/s^2)	Peak Damper Force (N)
El Centro (50%)	Uncontrolled	-	0.118	0.018	5.513	–
	One SMA-TSD	n = 40; Φ = 0.1 mm; L = 0.22 m	0.107 (–9.32)	0.017 (–5.56)	6.720 (21.89)	341.41
	Two SMA-TSD	n = 40; Φ = 0.1 mm; L(GS) = 0.14 m; L(FS) = 0.29 m	0.070 (–40.68)	0.010 (–44.44)	3.571 (–35.23)	78.95 (GS) 279.23 (FS)
El Centro (100%)	Uncontrolled	–	0.236	0.036	11.017	–
	One SMA-TSD	n = 50; Φ = 0.58 mm; L = 0.2 m	0.167 (–29.24)	0.029 (–19.44)	9.741 (–11.58)	1746.20
	Two SMA-TSD	n = 50; Φ = 0.58 mm; L(GS) = 0.14 m; L(FS) = 0.29 m;	0.110 (–53.39)	0.018 (–50.00)	7.976 (–27.61)	157.80 (GS) 1338.40 (FS)
El Centro (150%)	Uncontrolled	–	0.354	0.054	16.530	–
	One SMA-TSD	n = 70; Φ = 0.58 mm; L= 0.25 m	0.258 (–27.12)	0.045 (–16.67)	15.107 (–8.61)	2946.70
	Two SMA-TSD	n = 70; Φ = 0.58 mm; L(GS) = 0.18 m; L(FS) = 0.36 m	0.168 (–52.54)	0.029 (–46.67)	12.459 (–24.63)	238.86 (GS) 2377.80 (FS)
Kobe (50%)	Uncontrolled	–	0.291	0.054	18.561	-
	One SMA-TSD	n = 16; Φ = 0.58 mm; L(GS) = 0.18 m	0.308 (5.84)	0.048 (–11.11)	17.168 (–7.51)	2977.00
	Two SMA-TSD	n = 15; Φ = 0.58 mm; L(GS) = 0.97 m; L(SS) = 0.23 m	0.264 (–9.28)	0.045 (–16.67)	15.058 (–18.87)	8878.00(GS) 6295.60 (SS)

Note: [1] TSD design parameters: n = nos. of SMA slings, Φ = diameter of SMA slings, L = length of SMA slings, GS = ground storey, FS = first storey and SS = second storey

Author pl. check symbol is missing

seismic excitations except El Centro seismic excitation with 50% level, where peak acceleration is found to be shot up by 4└ 22%. Figure 4 shows peak interstorey drift response of uncontrolled and controlled ten-storey building. It is evident that control is most recently achieved across each storey for El Centro seismic excitations of 100% and 150% level but not 50% El Centro excitation and 50% Kobe seismic excitation. Peak acceleration plotted against each storey in Figure 5, reveals that one SMA-TSD

Figure 4: Peak Interstorey Drift for Ten-Storey Shear Building

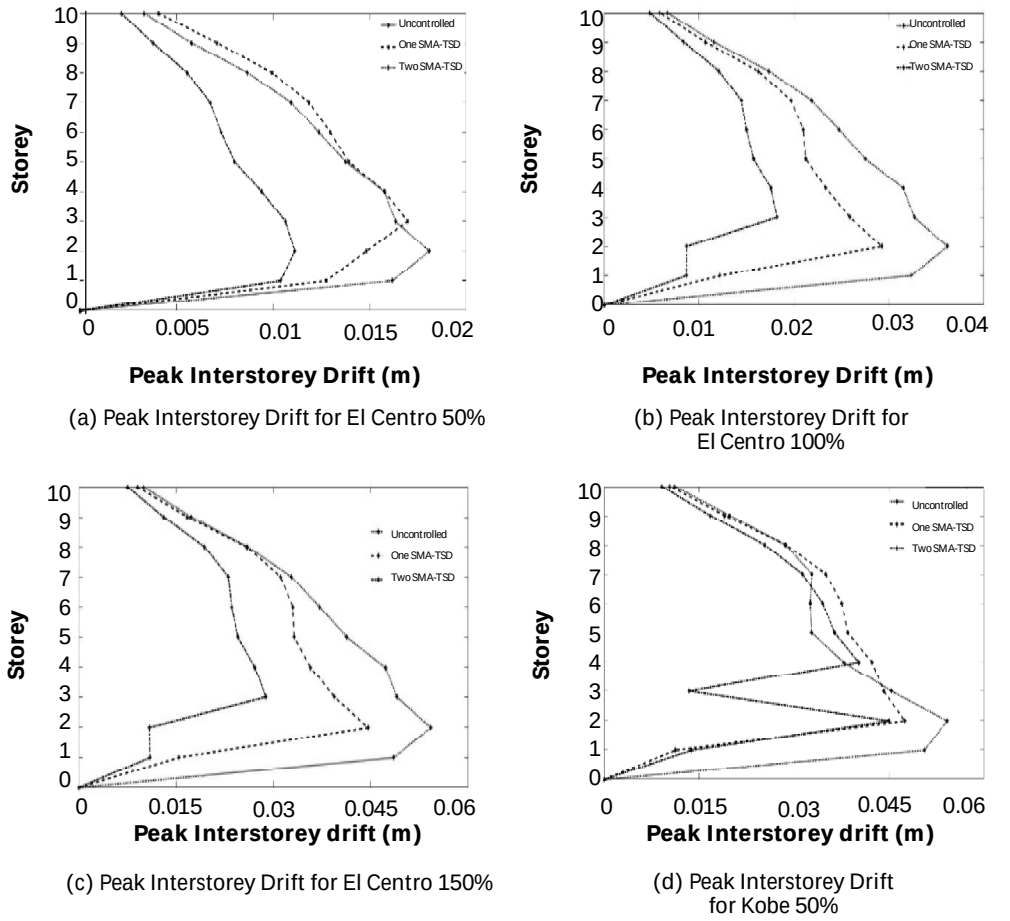

(a) Peak Interstorey Drift for El Centro 50%

(b) Peak Interstorey Drift for El Centro 100%

(c) Peak Interstorey Drift for El Centro 150%

(d) Peak Interstorey Drift for Kobe 50%

effectively controls acceleration almost every floor barring few exceptions under all seismic excitations. Reduction in seismic response parameters for ten-storey building with one SMA-TSD is attributed to supplemental damping offered by superelastic SMA wire which ranged between 13 and 21% under various seismic excitations.

3.2 Controlled Building with Two SMA-TSD

It is seen that seismic response parameters are mostly controlled by utilizing one SMA-TSD with ten-storey shear building. However, peak interstorey drift and peak accelerations at few storeys are not being controlled. Therefore, one more SMA-TSD is fitted between first and second storey of the ten-storey shear building. Placement of SMA-TSD in the building is decided referring to peak interstorey drift response of uncontrolled building. Controlled building, now fitted with two SMA-TSD, as shown

Figure 5: Peak Acceleration for Ten-Storey Shear Building

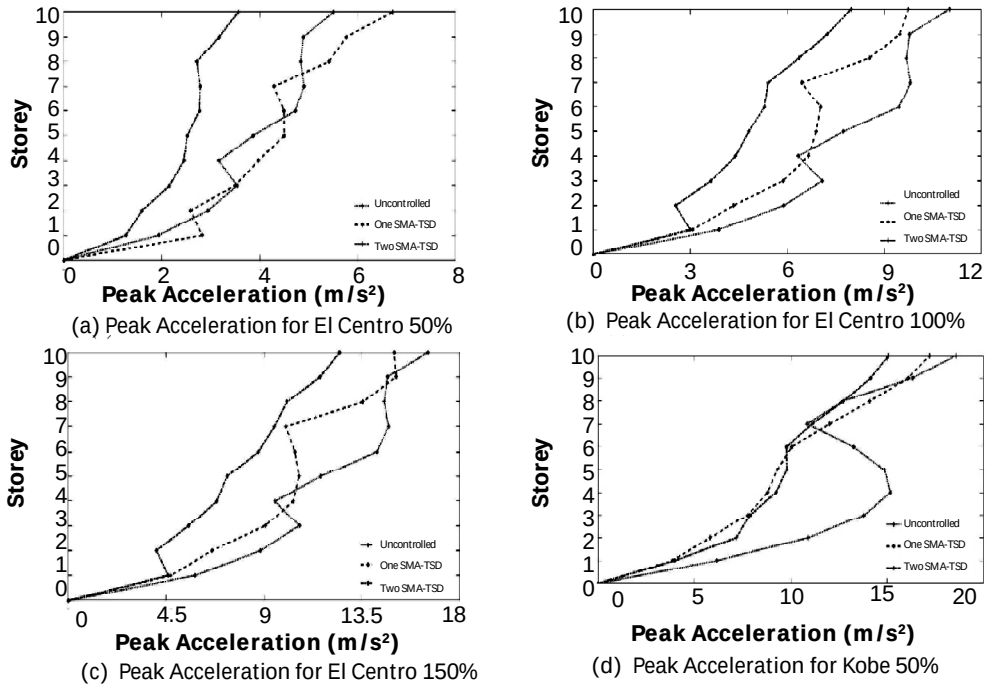

(a) Peak Acceleration for El Centro 50%

(b) Peak Acceleration for El Centro 100%

(c) Peak Acceleration for El Centro 150%

(d) Peak Acceleration for Kobe 50%

in Figure 1C, is subjected to different levels of El Centro seismic excitations and 50% Kobe seismic excitation. Design parameters of SMA-TSD has been kept same as that of derived for one SMA-TSD, so efficacy of two SMA-TSD is distinctly visible. Table 2 shows seismic response parameters of controlled building with two SMA-TSD under various seismic excitations. Bracketed quantity shows percentage difference between controlled and uncontrolled seismic response; –ve sign shows reductions. It is clearly evident that two SMA-TSD yields substantial reduction (4 53%) in peak displacement, interstorey drift and acceleration vis-à-vis uncontrolled building for different levels of El Centro seismic excitations. However, for 50% Kobe seismic excitations, seismic response control is moderate (4 19%) since higher vibration modes are excited under this seismic excitation.

Author pl. check symbols are missing

It is important to note here that two SMA-TSD outperforms one SMA-TSD in terms of seismic response control. The comparison among these passive dampers made possible as diameter and number of SMA tension slings are kept unchanged. However, length of SMA tension slings are altered to ensure maximum strain produced in them due to applied stress remains well within the maximum permissible strain of 6%. This restriction of induced strain in SMA wire prevents permanent deformation of SMA-wire from its original equilibrium position, i.e.,

no divergence from its base line. On the other hand, it limits damping capabilities of SMA-wire in SMA-TSD and thus remain slightly underutilized towards seismic response control.

Figure 4 shows peak interstorey drift plotted for ten-storey shear building with two SMA-TSD for each seismic excitation. It is evident that SMA-TSDs efficiently reduces peak interstorey drift for each storey of the building for different levels of El Centro seismic excitations when they are fitted at bottom two storeys. However, it has been found that the said placement of SMA-TSDs could not control the peak interstorey drift for upper storeys for 50% Kobe seismic excitation. Thus, SMA-TSD placements are rearranged with one SMA-TSD at bottom storey and other between second and third storey to achieve better seismic control. Peak acceleration at each storey for the same building is plotted in Figure 5. It is evident that two SMA-TSD yields substantial reduction at each storey of controlled building vis-à-vis uncontrolled building under all seismic excitations.

Time history plot for interstorey drift at second storey of the uncontrolled and controlled buildings (with one and two SMA-TSD) are given in Figure 6 for each seismic excitation accounted for. It is revealed that both SMA-TSD (one and two) show good interstorey drift control throughout time extent of seismic excitations. It is evident that controlled buildings creep back to its base line without any offset. Two SMA-TSD outperforms one-TSD performance in reducing peak seismic response

Figure 6: Interstorey Drift at Second Storey Level of Ten-Storey Shear Building

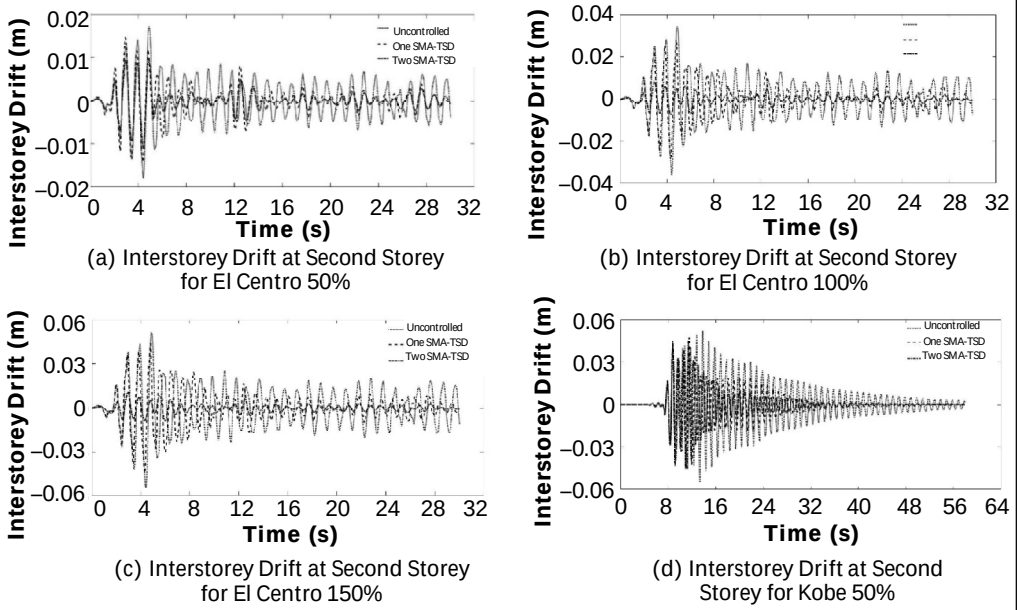

(a) Interstorey Drift at Second Storey for El Centro 50%

(b) Interstorey Drift at Second Storey for El Centro 100%

(c) Interstorey Drift at Second Storey for El Centro 150%

(d) Interstorey Drift at Second Storey for Kobe 50%

quantities and controlling response throughout time history. Table 2 shows peak damper force magnitude increases with levels of seismic excitations with highest damping force offered by SMA-TSD for Kobe seismic excitations. The study reveals that pulse type Kobe seismic excitation requires relatively larger length of SMA tension slings for passive seismic response control as compared to El Centro seismic excitation.

Conclusion

In this paper, ten-storey shear building is fitted with one and two SMA-TSD to passively control its seismic response. El Centro seismic excitations with 50%, 100% and 150% levels and 50% Kobe seismic excitations are considered. Behavior of SMA-TSD is characterized by Tanaka model considered with isothermal conditions. Equivalent linear model for SMA-TSD is developed using Voigt model of linear dynamic theory for viscoelastic material with memory effects. Passive damper force is represented with two components of stiffness and viscous damping characterized for each seismic excitation considered in the study. Uncontrolled seismic response of ten-storey shear building is evaluated and is compared with controlled buildings fitted with one SMA-TSD and two SMA-TSD. Seismic parameters, peak displacement, interstorey drift, acceleration and peak damper force are evaluated. Design parameters of SMA-TSD, diameter, length and number of SMA tension slings are determined through iterative search method. It has been found that one SMA-TSD yields moderate seismic response control for El Centro seismic excitation of 100% and 150% levels. Controlled building with two SMA-TSD very effectively controls seismic response for all seismic excitations and outperforms one SMA-TSD. SMA-TSD is slightly underutilized towards seismic response control due to constraint imposed on it for maximum strain. Seismic parameters of superelastic SMA-based TSD can be optimized to yield better seismic response control.

References

Author pls provide missing volume and issue numbers for 1, 6, 10, 12, 15, 16, 21, 24, 25, 26, 30, 31 and 32 references

1. Aiken I D and Kelly J M (1992), "Comparative Study of Four Passive Energy Dissipation Systems", *Bulletin of New Zealand Society for Earthquake Engineering*, Vol. 25, pp. 175-192.
2. American Association of State Highway and Transportation Officials, Guide Specifications for Seismic Isolation Design (1991), Washington DC.
3. Boyd J D and Lagoudas D C (1996), "A Thermodynamical Constitutive Model for Shape Memory Materials Part I: The Monolithic Shape Memory Alloy", *International Journal of Plasticity*, Vol. 12, No. 6, pp. 805-842.
4. Buehler W and Wiley R (1961), Nickel Based Alloys, Patent US3174851A.
5. Chen G, Garret G T, Chen C and Cheng F Y (2004), "Piezoelectric Friction Dampers for Earthquake Mitigation of Buildings: Design, Fabrication and

Characterization", *Structural Engineering and Mechanics*, Vol. 17, Nos. 3&4, pp. 539-556.

6. Dolce M, Cardone D, Ponzo F and Valente C (2005), "Shaking Table Tests on Reinforced Concrete Frames Without and With Passive Control Systems", *Earthquake Engineering and Structural Dynamics*, Vol. 34, pp. 1687-1717.
7. Fan Y, Sun K, Zhao Y *et al*. (2019), "A Simplified Constitutive Model of Ti-Ni SMA with Loading Rate" , *Journal of Materials Research and Technology*, Vol. 8, No. 6, pp. 5374-5383.
8. Ghodke S and Jangid S (2016), "Equivalent Linear Elastic-Viscous Model of Shape Memory Alloy for Isolated Structures", *Advances in Engineering Software*, Vol. 99, No. 22, pp. 1-8.
9. Graesser E and Cozzarelli F (1991), "Shape Memory Alloys as New Materials for Seismic Isolation", *Journal of Engineering Mechanics*, Vol. 117, No. 11, pp. 2590-2608.
10. Hartl D J and Lagoudas D C (2008), "Shape Memory Alloys: Modelling and Engineering Applications", *Springer Science*, pp. 53-119.
11. Housner G W, Bergman L A, Caughey T K *et al*. (1997), "Structural Control: Past, Present and Future", *Journal of Engineering Mechanics*, Vol. 123, No. 9, pp. 898-971.
12. Jani J M, Leroy M, Subik A and Gibson M (2014), "A Review of Shape Memory Alloy Research, Applications and Opportunities", *Materials and Design*, Vol. 56, pp. 1078-1114.
13. Jansen L M and Dyke S J (1999), "Semi-Active Control Strategies for MR Dampers: A Comparative Study", *Journal of Engineering Mechanics*, Vol. 126, No. 8, pp. 795-803.
14. Liang C and Rogers C A (1997), "One-Dimensional Thermomechanical Constitutive Relations for Shape Memory Materials", *Journal of Intelligent Material Systems and Structures*, Vol. 8, No. 4, pp. 285-302.
15. McCormik J, DesRoches R, Fugazza D and Auricchio F (2006), "Seismic Vibration Control Using Superelastic Shape Memory Alloys", *Journal of Engineering Materials and Technology,* Vol. 128, pp. 294-301.
16. Miller D J, Fahnestock L and Eatherton M (2012), "Development and Experimental Validation of a Nickel - Titanium Shape Memory Alloy Self Centering and Buckling Restrained Braces", *Engineering Structures*, Vol. 40, pp. 288-298.

17. Mortazavi S M R, Ghassemieh M and Motahari S A (2013), "Seismic Control of Steel Structures with Shape Memory Alloys", *International Journal of Automation and Control Engineering*, Vol. 2, No.1, pp. 28-34.

18. Ozbulut O E, Hurlebaus S and Desroches R (2011), "Seismic Response Control Using Shape Memory Alloys: A Review", *Journal of Intelligent Material Systems and Structures*, Vol. 22, No. 14, pp. 1531-1549.

19. Ozdemir H (1976), "Nonlinear Transient Dynamic Analysis of Yielding Structures", PhD Dissertation, University of California at Berkeley, Berkeley, CA.

20. Pall A S and Marsh C (1982), "Seismic Response of Friction Damped Braced Frames", *Journal of Structural Engineering, ASCE*, Vol. 108, No. 6, pp. 1313-1323.

21. Purohit S P and Chandiramani N K (2012), "Semi-Active Control Using Magneto-Rheological Dampers with Output Feedback and Distributed Sensing", *Shock and Vibrations*, Vol. 19, pp. 1427-1443.

22. Ren W, Li H and Song G (2007), "A One-dimensional Strain-Rate-Dependent Constitutive Model for Super-Elastic Shape Memory Alloys", *Smart Mater Struct*, Vol. 16, No. 1, pp. 191-197.

23. Sae-Ung S and Yao J T P (1978), "Active Control of Building Structures", *Journal of the Engineering Mechanics*, Vol. 104, No. 2, pp. 335-350.

24. Schmidt I (2006), "A Phenomenological Model for Super-Elastic NiTi Wires Based on Plasticity with Focus on Strain-Rate Dependency Caused By Temperature", *Journal of Engineering Material and Technology*, Vol. 128, pp. 279-284.

25. Soong T T and Spencer B F (2002), "Supplementary Energy Dissipation: State-of-the-Art and State-of-the-Practice", *Engineering Structures*, Vol. 24, pp. 243-259.

26. Spencer B F and Nagarajaiah S (2003), "State of the Art Structural Control", *Journal of Structural Engineering, ASCE*, Vol. 129, pp. 845-856.

27. Sun C T and Lu Y P (1995), *Vibration Damping of Structural Elements*, Prentice Hall Series, Pearson Publications, ISBN: 0130792292.

28. Symans M D and Constantinou M C (1998), "Passive Fluid Viscous Damping Systems for Seismic Energy Dissipation", *Journal of Earthquake Technology*, Vol. 35, No. 4, pp. 185-206.

29. Symans M D, Charney F A, Whittaker A S *et al*. (2008), "Energy Dissipation Systems for Seismic Applications: Current Practice and Recent Developments", *Journal of Structural Engineering, ASCE*, Vol. 134, No. 1, pp. 4-21.

30. Tanaka K A (1986), "Thermomechanical Sketch of Shape Memory Effect: One-Dimensional Tensile Behaviour", *Research Mechanical*, Vol. 18, pp. 251-263.

31. Yuen K, Shi Y, Beck J and Lam H (2007), "Structural Protection Using MR Dampers with Clipped Robust Reliability-Based Control", *Struct Multidisc Optim*, Vol. 34, pp. 431-443.

32. Zhang Y and Zhu S (2007), "A Shape Memory Alloy-Based Reusable Hysteretic Damper for Seismic Hazard Mitigation", *Smart Materials and Structures*, Vol. 16, pp. 1603-1613.

Reference # 62J-2021-01-0x-01